### Title
Real-time measurement of sodium in single aerosol particles by flame emission: laboratory characterization




### Journal
Journal of Aerosol Science, 32(6)

### ISSN
0021-8502



### Authors
Clark, Catherine D
Campuzano-Jost, Pedro
Covert, David S
et al.



### Publication Date
2001-06-01

### DOI
10.1016/s0021-8502(00)00120-8

PERGAMON

Aerosol Science 32 (2001) 765–778

Journal of
Aerosol Science

www.elsevier.com/locate/jaerosci

# Real-time measurement of sodium in single aerosol particles by flame emission: laboratory characterization

Catherine D. Clark[a], Pedro Campuzano-Jost[b], David S. Covert[c], Robert C. Richter[d], Hal Maring[b], Anthony J. Hynes[b], Eric S. Saltzman[e,*]

[a]*Department of Environmental and Chemical Sciences, Chapman University, One University Drive, Orange, CA 92866, USA*
[b]*Division of Marine and Atmospheric Chemistry, Rosenstiel School of Marine and Atmospheric Sciences, University of Miami, 4600 Rickenbacker Causeway, Miami, FL 33149, USA*
[c]*Department of Atmospheric Sciences, University of Washington, Seattle, WA 98195-1750, USA*
[d]*Sincotrone Trieste, I-34012 Trieste, Italy*
[e]*Department of Earth System Science, University of California, Irvine, 220 Rowland Hall, Irvine, CA 92697-3100, USA*

Received 25 May 2000; received in revised form 20 November 2000; accepted 22 November 2000

**Abstract**

A flame emission aerosol sodium detector (ASD) has been developed to study the distribution of seasalt in individual marine aerosol droplets. The instrument detects sodium via D-line emission in a fuel-rich, laminar, hydrogen/oxygen/nitrogen flame. Laboratory studies with synthetic monodisperse aerosols were carried out in order to characterize the sensitivity, precision, and linearity of the technique. Experiments were also carried out with aerosols generated from mixed salt solutions and seawater in order to determine whether ionic or other matrix effects lead to interference. The ASD has a linear response function for NaCl aerosol particles from 100 nm to 2.0 μm in diameter. The precision of sodium mass measurements is on the order of $\pm$ 3% standard error on replicate measurements, with a quantitative response to the sodium content of a single aerosol particle that is independent of the chemical composition of the particle, i.e. anions, cations, seawater. No interferences were found with major ions in seawater and common atmospheric aerosols. These experiments demonstrate a detection limit equivalent to a 100 nm diameter dry 100% NaCl aerosol.


*Keywords:* Sea salt; Sodium flame emission; Single-particle analysis; Marine aerosols

* Corresponding author.
*E-mail addresses:* cclark@rsmas.miami.edu (C.D. Clark), pedro@rsmas.miami.edu (P. Campuzano-Jost), dcovert@u.washington.edu (D.S. Covert), robert.richter@elettra.trieste.it (R.C. Richter), hmaring@rsmas.miami.edu (H. Maring), ahynes@rsmas.miami.edu (A.J. Hynes), esaltzma@uci.edu (E.S. Saltzman).

0021-8502/01/$ - see front matter 
PII: S0021-8502(00)00120-8

## 1. Introduction

Seasalt aerosol particles are an important component of marine air affecting both physical processes, such as light scattering and cloud droplet growth, and chemical process involving the uptake and release of reactive gases (Livingston & Finlayson-Pitts, 1991; Chameides & Stelson, 1992; Sievering et al., 1992; Keene et al., 1998). Seasalt particles are produced at the ocean surface by the bursting of entrained air bubbles produced by the action of wind (Woodcock, 1953; Blanchard & Woodcock, 1957, 1980; Blanchard, 1983; Monahan, Spiel, & Davidson, 1986; Gong, Barrie, Blanchet, & Spacek, 1998). Mechanical generation typically produces particles ranging from 0.1 to 100 μm in diameter. The production rate of sub-micron primary seasalt particles is poorly known. Although non-seasalt (nss) sulfate particles have traditionally been considered to dominate this size range based on early measurements (for example, Hobbs, 1971), recent indirect evidence has suggested that sub-micron seasalt production may, in fact, be significant (O'Dowd & Smith, 1993; O'Dowd, Smith, Consterdine, & Lowe, 1997). More recently, single aerosol mass spectrometer measurements at Cape Grim, Tasmania, showed that nearly all particles larger than 0.13 μm in diameter contained seasalt, and seasalt was a significant fraction of the CCN (Murphy et al., 1998a,b). To resolve the relative contribution of seasalt aerosol particles to number and mass distributions in the sub-micron size range, more direct quantitative measurements of sodium levels in ambient single aerosol particles under a wide range of wind speeds and local conditions are clearly needed.

One approach to measuring sodium quantitatively is flame spectrometry. This technique has been extensively used in the past to analyze nebulized solutions of sodium salts in both laminar and turbulent flames (Alkemade & Herrmann, 1979a). Numerous experimental studies have demonstrated a linear relationship between the integrated intensity of absorption, fluorescence and emission and the concentration of ground state atoms, provided that the optical density, i.e. atomic concentration, is low (Zeegers, Smith, & Winefordner, 1968). At high concentrations, the relationship is no longer linear due to self-absorption effects in optically thick flames (Zeegers et al., 1968). Other causes of non-linear behavior include incomplete desolvation and volatilization of the nebulized droplets in the flame, and incomplete dissociation of the salts to give free sodium atoms (Alkemade & Herrmann, 1979b,c).

A variety of flames have been used in analytical flame spectroscopy studies, ranging from acetylene/air to hydrogen flames (Alkemade & Herrmann, 1979a). A hotter flame reduces potential problems with incomplete volatilization and dissociation. Early studies showed that sodium emission in a hydrogen flame is practically the same for all sodium halides and other sodium salts (Alkemade & Herrmann, 1979a). More recently, many researchers have studied the chemistry of sodium in hydrogen/air flames of varying composition in great detail (e.g. Hynes, Steinberg, & Schofield, 1984). These studies all utilized steady-state flame concentrations resulting from the large numbers of droplets produced by nebulizing solutions.

There have been very limited measurements of sodium in flames from *single* aerosol particles. One early device counted sodium-containing atmospheric aerosol particles when they entered a hydrogen flame (Soudain, 1951; Vonnegut & Neubauer, 1953). This system used turbulent flames on two burners for large and small particles. Aerosol particles were entrained with the air flow into both flames, with transmission efficiencies less than 10%. This system was subject to large fluctuations in background signal from the turbulent flames, masking signals from small particles.

The system overall had very low sensitivity, with an estimated detection limit of 1 μm diameter particles (Vonnegut & Neubauer, 1953). This apparatus was not calibrated to give a quantitative response, but simply used as a sodium counter.

A later variation of the salt counter incorporated an acetylene pre-mixed laminar flat flame to ensure all particles would traverse the same temperature profile (Radke & Hobbs, 1969). In this instrument, atmospheric aerosol particles were also sampled by entrainment into the air flow drawn in by the burner at a rate that ensured proper burning. Since particles were introduced into the flame over the entire burner head region and would most likely not be imaged evenly by the detection optics, reproducibility was probably poor. An improved version of this sodium flame spectrometer was later flown over the Pacific ocean (Hobbs, 1971). Sodium particles in the range 0.06–0.68 μm diameter of equivalent dry NaCl particles were measured, with very low sodium particle counts above 0.23 μm. No details on instrument calibration, precision or design changes to the 1969 version were given.

A sodium-particle counter was most recently deployed on several flights off the east coast of the US in 1993 (Hegg, Hobbs, Ferek, & Waggoner, 1995). This system used a flame photometric detector with a reducing hydrogen/air flame, coupled to a pulse height analyser, to measure sea salt size distributions between 0.1 and 5 μm in diameter. The instrument was calibrated with NaCl particles generated by an atomizer/electrostatic classifier, but precision and transmission efficiencies are not reported. Seasalt particle concentrations in this study ranged from 0.2 to 2 $cm^{-3}$, comprising just a few percent of the sub-micron aerosol particles.

We have developed an improved aerosol sodium detector (ASD), which is designed to detect and quantify sodium in single aerosol particles from 100 nm to 2.0 μm with high precision, via thermal emission in a hydrogen/air flame. In this paper, we describe the design and operational principles of the instrument and present the results of laboratory tests with monodisperse aerosols to characterize its performance in terms of linearity of response, precision, sensitivity and potential chemical interferences. Some preliminary measurements on ambient aerosols from marine air are also presented.

## 2. Experimental methodology

### 2.1. *The aerosol sodium detector* (*ASD*)

The basic principles of operation of the ASD are the volatilization of aerosol particles in a high-temperature flame, decomposition of the sodium salts to give sodium atoms, and detection of the emission at 589.0 ($D_2$ line) and 589.6 nm ($D_1$ line) from thermally excited sodium atoms. The ASD consists of the following components: (1) an aerosol sampling and injection system to introduce aerosol particles into the flame, (2) a pre-mixed laminar hydrogen/air flame for volatilization of the aerosol and atomization of sodium salts, and (3) a PMT, sodium filter and associated electronics for data acquisition. A schematic of the ASD is shown in Fig. 1 and each of its components is discussed in more detail below. Unlike the earlier versions of sodium aerosol flame spectrometers (Soudain, 1951; Vonnegut & Neubauer, 1953; Radke & Hobbs, 1969), aerosol particles in the ASD are introduced reproducibly into the center of the laminar flat flame through the aerosol inlet capillary. All sampled aerosol particles traverse the same region imaged by the optical detectors, giving high precision sodium emission measurements.

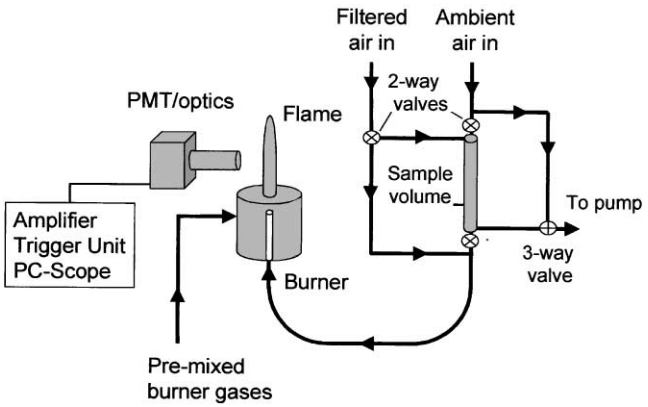


Fig. 1. Simplified schematic of the Aerosol Sodium Detector (ASD; not to scale).

### 2.2. Aerosol sampling

Aerosols are sampled by drawing air at 1 $l\,min^{-1}$ through a system of electronically controlled on/off valves into a copper collection tube 53 cm long by $\frac{3}{8}''$ (9.5 mm) OD. An early version of the ASD sampled air directly into the burner induced by pumping on a sealed chamber surrounding the burner head. This proved unsuccessful due to instabilities in the aerosol flow. In the final configuration of the ASD, the collected sample is periodically injected into the flame front through the aerosol inlet capillary under pressure with filtered laboratory compressed air (0.25 $l\,min^{-1}$). During a sampling cycle, the compressed air bypasses the sampling tube and enters the flame front directly (Fig. 1). Valve switching is controlled and monitored by the data acquisition program. To minimize particle losses by impaction, the aerosol flow path is unobstructed and sharp bends in tubing were avoided. Particle transmission efficiencies through the sampling/injection system are estimated to be $> 95\%$ for particles below 2 μm in diameter based on calculated particle settling velocities and residence times for the flow rates used in this system (Reynolds number = 147; Stokes number = 0.084; residence time = 3 s; settling velocity for 2 μm particle = 0.0261 $cm\,s^{-1}$).

### 2.3. Burner

The ASD burner consists of a machined aluminum body incorporating a stainless-steel honeycomb head 0.5″ (1.27 cm) in diameter that can be easily removed for cleaning. A simplified schematic of the burner is shown in Fig. 2. The flame gas flow rates used in the laboratory study were 3.0 $l\,min^{-1}$ hydrogen, 5.8 $l\,min^{-1}$ air, and 3.4 $l\,min^{-1}$ nitrogen, giving a stable fuel-rich flame with a temperature $\sim$1600 K. A fuel-rich hydrogen/air flame minimizes the formation of NaOH and $NaO_2$ which result in a net loss of elemental sodium from the system (Hynes et al., 1984). The colorless laminar flame is $\sim$7 cm in height, with a 2 mm high bright blue zone at its base. A nitrogen sheath flow of 2.2 $l\,min^{-1}$ around the honeycomb head minimizes entrainment of aerosol particles from the room air. All gases are filtered with HEPA capsule filters. The aerosols are introduced at a flow rate of 0.25 $l\,min^{-1}$ into a well-defined central region of the flame through

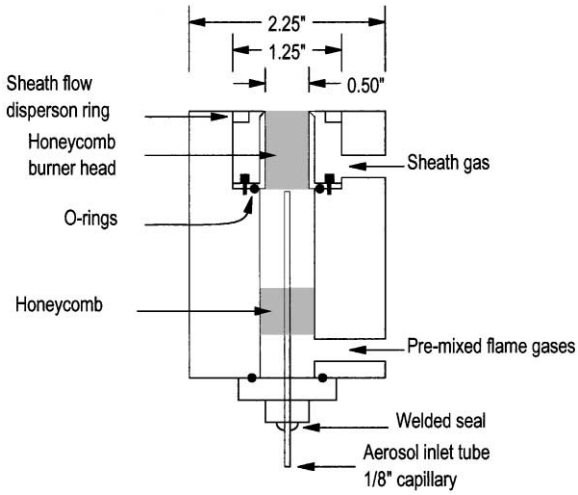


Fig. 2. Simplified schematic of the ASD burner (not to scale).

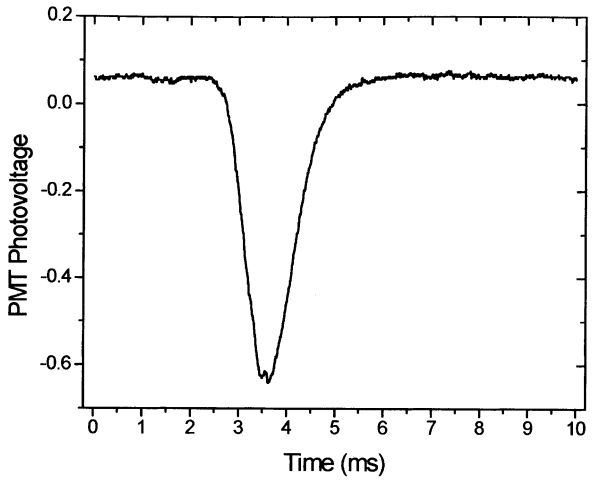


Fig. 3. PMT photovoltage vs. time (ms) for a single 1.25 μM aerodynamic diameter NaCl aerosol particle.

a capillary tube. The linear velocities of the aerosol and pre-mixed flame gas flows below the burner head are matched to ensure laminar flow conditions and minimize particle losses from turbulence.

### 2.4. Signal detection and data acquisition

The light emitted from the thermally excited sodium atoms at 589.0/589.6 nm ($^2P_{3/2}$ and $^2P_{1/2}$ Na doublet) is imaged by a telescope (consisting of iris, mask, two lenses, a sodium interference filter) and detected with a 1P28 photomultiplier tube (Hamamatsu). A 10 nm broad-band filter was used for the linearity and precision experiments discussed below in section 3.1. For

all subsequent experiments a 0.1 nm narrow line filter was used, reducing sodium signal by a factor of approximately 3.4. The narrow line filter reduced the sodium signal by a factor of approximately 3.4 relative to the broad-band filter. The telescope is used to image a roughly cylindrical volume approximately 6 mm in diameter, which intersects the flame (approximately 12.6 mm diameter), 2 cm above the burner head. The response of the instrument to a given mass of sodium varied during the course of this study because of changes in iris diameter and PMT alignment. Each individual experiment was carried out under a single set of conditions, but it is not meaningful to compare the absolute magniture of the response between different experiments. The PMT signal is passed to an adjustable gain, high-input impedance amplifier, and recorded using a PC-based oscilloscope board. Data acquisition is triggered by the emission signal. The duration of a sodium signal from a single particle is approximately 2 ms. Fig. 3 is a plot of the signal acquired from a single 1.25 μm diameter NaCl aerosol. System "background" signals are collected by running the aerosol inlet flow to the flame through a filter and setting the delay generator to internally trigger.

Data analysis consists of integrating the area of the sodium emission peak relative to the baseline PMT signal. These peak areas are normalized by the gain of the signal amplifier. Aerosol acquisitions with multiple aerosol events in a single shot are discarded to avoid errors in the calculated areas. As a measure of the precision of the emission signal, the standard error of the mean peak area for a measurement of 100 monodisperse aerosol particles is typically $\pm 3\%$ ($2\sigma$).

### 2.5. Calibration

The ASD is calibrated with monodisperse aerosols of known sizes, produced by a vibrating orifice aerosol generator (VOAG; John, 1993). Aqueous salt solutions ranging from 0.2 to $4 \times 10^{-4}$ M are forced through a 20 μm platinum orifice by a nitrogen backing pressure of 40 Psi (240 kPa). All sodium salts are standard purity from Aldrich. Salts are dried for at least 24 h at 100°C and cooled in a vacuum dessicator prior to solution preparation in deionized MilliQ water. The orifice is vibrated by a piezo electrode with a square wave pulse (frequency = 272.5 kHz; amplitude = 30 V) to break up the liquid stream, producing large monodisperse droplets. The droplets are entrained in an air flow of 1.75 l $min^{-1}$ to prevent coagulation. The droplets are then dried in a column with dry filtered compressed air (10 l $min^{-1}$), and sized with a commercial aerodynamic particle sizer (TSI 3310A; Baron, Mazunder, & Cheng, 1993).

The initial size of the droplet as a geometric diameter produced by the VOAG can be calculated from (John, 1993)

$$D_d = (6Q/\pi f)^{1/3}, \tag{1}$$

where $f$ is the frequency of orifice vibration (s), $Q$ is the liquid flow rate ($cm^3\ s^{-1}$) and $D_d$ is the droplet diameter (cm). For the current set of operating conditions, the frequency is 272.5 kHz, and the flow rate was measured at 0.4 $cm^3\ min^{-1}$, giving an initial geometric droplet diameter of 37 μm. The final size of the particles generated in these experiments varied from 0.8 to 2 μm in diameter, depending on the composition (i.e. density of the salt) and initial concentration of the salt solutions used. The sodium mass contained in a single aerosol is calculated from the initial sodium concentration, the initial droplet volume and the molar mass of sodium. In the experiments described here, sodium levels ranged from 0.004 to 0.24 pg in a single aerosol particle. The accuracy of the sodium calibration is dependent on the calculation of the initial droplet volume. The largest

source of uncertainty in the calculated initial droplet size lies in the liquid flow-rate measurement, giving a potential systematic error of $\pm 10\%$ in droplet volume.

### 2.6. Field setup for ambient measurements

In April 2000 during the Shoreline Environment Aerosol Study (SEAS), ambient aerosols were sampled through an aerosol intake system on the tower at the University of Hawaii's meteorological research site at Bellows air force base on the southeast coast of Oahu, Hawaii. The aerosol intake was located at 12 m above sea level and consisted of a $\frac{1}{2}''$ (1.27 cm) OD goose-neck stainless-steel tube facing into the prevailing winds. The inlet was connected to $\frac{3}{8}''$ (9.52 mm) OD black, high-carbon-content plastic tubing (TSI) run vertically down to the ASD. A pump drew outside air through the inlet tube at a rate of 11 l $\mathrm{min}^{-1}$ (Reynolds number = 1219; residence time = 10 s; Stokes number = 0.18, calculated for a 4.8 μm particle — 50% cut point at 0.47 for a round tube inlet). Inside the laboratory, a smaller flow (0.4 l $\mathrm{min}^{-1}$) was iso-kinetically drawn off from the main flow through a $\frac{1}{8}''$ (3.18 mm) OD stainless-steel capillary into a 122 cm long, $\frac{1}{4}''$ (6.35 mm) diameter PVC Nafion drying tube (counter-air drying flow = 0.8 l $\mathrm{min}^{-1}$; Reynolds number = 267; residence time = 0.24 s; Stokes number = 0.34). This ran directly to the intake of the aerosol injection system. Measurements with an aerodynamic particle sizer (APS; TSI) demonstrated $>95\%$ transmission of all aerosol particles $<2$ μm in diameter through the sampling system. For these ambient aerosol experiments, a smaller, 0.25″ (6.35 mm) OD burner head and correspondingly lower flame gas and aerosol injection flows were used ($H_2 = 1.23$ l $\mathrm{min}^{-1}$; $N_2 = 0.6$ l $\mathrm{min}^{-1}$; air = 3.06 l $\mathrm{min}^{-1}$; sheath = 1.02 l $\mathrm{min}^{-1}$; aerosol = 0.117 l $\mathrm{min}^{-1}$). For the field experiment, a small chamber flushed by filtered air at 11 l $\mathrm{min}^{-1}$ was fitted around the burner head and detection optics to minimize entrainment of laboratory aerosol particles into the flame.

## 3. Results and discussion

### 3.1. Linearity of response/precision

In order to assess the linearity of the response of the ASD, a series of solutions of different NaCl concentrations were introduced into the VOAG. NaCl concentrations ranged from 0.12 to $3.08 \times 10^{-4}$ M NaCl, giving aerosol particles in the 0.9–2 μm diameter size range after conditioning in the drying column (aerodynamic diameters measured by the APS). The sodium content of these particles ranged from 0.006 to 0.18 pg. These dried particles are probably of irregular geometry and may consist of crystal aggregates. No attempt was made to measure sodium in larger aerosols due to the low system transmission efficiency above 2 μm. Fig. 4 shows emission signals as a function of sodium content for single aerosols. Emission signals were linear ($r = 0.998$), increasing with increasing sodium concentration as expected. The linearity of the response suggests that: (1) volatilization of the aerosols is complete, and (2) the flame remains optically thin (i.e. no evidence of self-absorption).

Standard errors for each point (corresponding to a $\sim 100$ particle data set) are shown as $y$-error bars in Fig. 4. Errors vary from 1.8 to 3.6%, with a mean value of 2.3%, demonstrating excellent

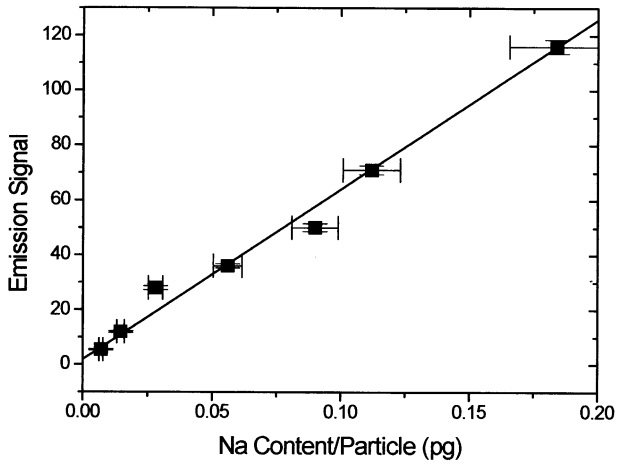


Fig. 4. Emission vs. sodium content for single monodisperse NaCl aerosol particles. Each point represents the mean of the integrated emission signal for approximately 100 particles. Error bars represent the standard error for sodium emission and $\pm$ 10% for sodium content/particle.

short-term precision. However, there were apparent departures from linearity that exceeded the uncertainty in the individual data sets. We believe these reflect variations in flame temperature resulting from drift in the flow rates of the flame gases, which were not mass flow controlled during these experiments. The response of the ASD would be expected to vary with flame temperature as a result of the temperature dependence of the Maxwell–Boltzmann distribution of sodium atoms in the $^2P_{3/2}$ and $^2P_{1/2}$ excited states in the flame.

To further probe the linearity of the system response, this experiment was repeated with a series of NaCl/KCl mixtures, ranging from 100% down to 4% v/v NaCl. In all cases, the total chloride concentration of the solutions was $1.65 \times 10^{-4}$ M, and the aerodynamic diameters of the aerosol particles measured by the APS were $1.3 \pm 0.2$ μm. Fig. 5 shows emission as a function of sodium content in single mixed NaCl/KCl aerosol particles. Again, the response function is linear within the flame temperature uncertainty from 0.004 to 0.10 pg Na in a single aerosol particle.

### 3.2. Chemical interferences

Although the atomic emission from sodium is quite specific, the chemical composition of the non-sodium components of the aerosol could affect the response of the ASD in a number of ways. For example, chemical composition might affect the rate of volatilization and decomposition of the sodium salts, and other aerosol constituents could affect the flame chemistry in such a way as to alter the abundance of atomic sodium relative to non-emitting forms such as sodium oxide. To determine if the sodium response of the ASD depends *only* on the amount of sodium present and *not* on the nature of the other chemicals present in the aerosol particle, the emission was measured for a series of sodium salts with anions that are important constituents of seawater and/or seasalt aerosols (NaBr, $NaNO_3$, $Na_2SO_4$ and $Na_2CO_3$). Salt concentrations for these experiments were 1, 2, 3, and $4 \times 10^{-4}$ M, giving monodisperse aerosol particles with sodium contents ranging from

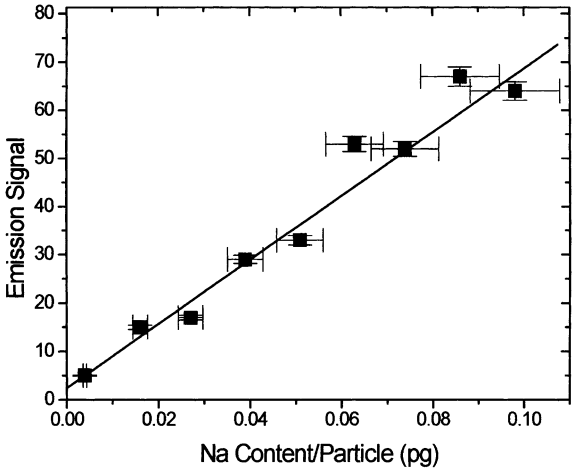


Fig. 5. Emission signals vs. sodium content (in pg) for mixed NaCl/KCl single aerosol particles. Error bars are $\sim 3\%$ standard error for sodium emission and $\pm 10\%$ for sodium content/particle.

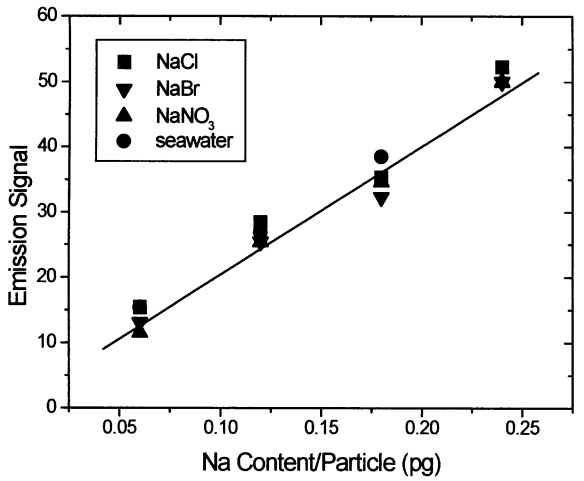


Fig. 6. Emission signals vs. sodium content (in pg) for single aerosol particles containing univalent sodium salts and seawater. Error bars are not shown for ease of viewing, but are $\sim 3\%$ for sodium emission and $\pm 10\%$ for sodium content/particle (as in Figs. 4 and 5).

0.06 to 0.24 pg, and 1–2 μm in diameter. Fig. 6 shows the results for NaBr and $NaNO_3$. NaCl is included for purposes of comparison. All three salts show a linear response with very similar sodium emission signals for single aerosol particles with the same sodium content, i.e. the sodium response is independent of the nature of the anion.

Divalent sodium salts also show a linear response for sodium. This is shown in Fig. 7a and b for $Na_2SO_4$ and $Na_2CO_3$, respectively. Again, this linear response indicates that there are no problems with complete volatilization and atomization of these salts in the flame. Since seawater largely consists of NaCl and $MgSO_4$, a mixture of these two salts was tested and also gave a linear

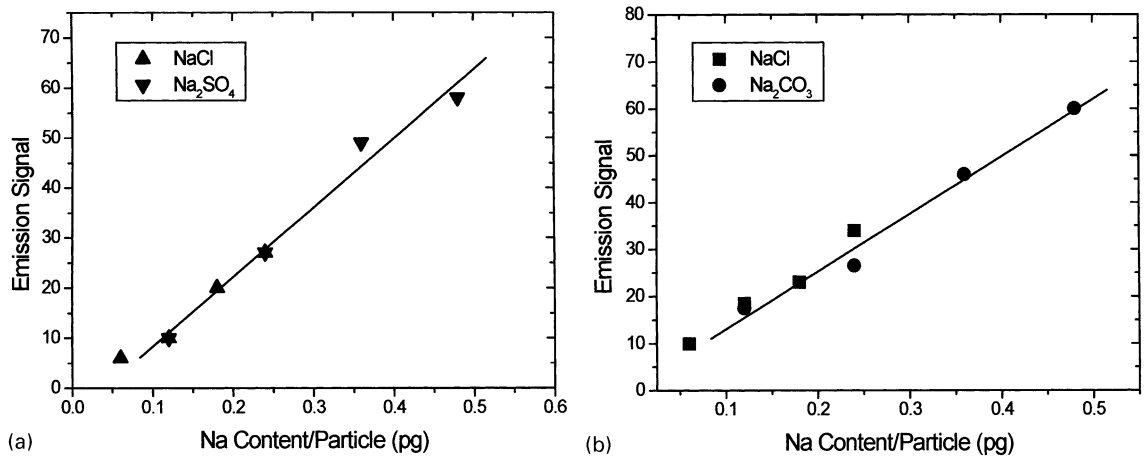


Fig. 7. Emission signals vs. sodium content (in pg) for divalent sodium salts in single aerosol particles Error bars are not shown, but are on the order of $\sim 3\%$ standard error for sodium emission and $\pm 10\%$ for sodium content/particle (as in Figs. 4 and 5).

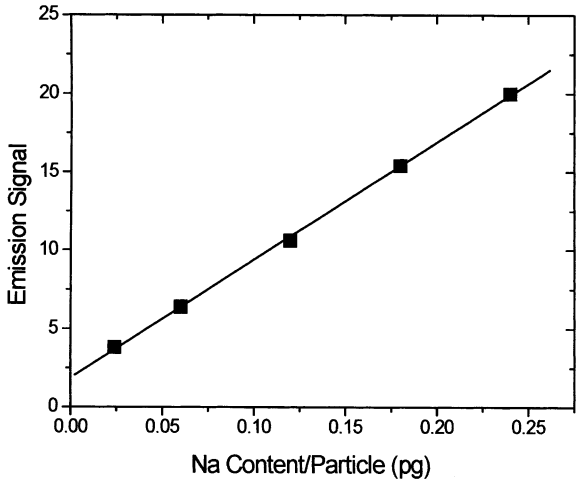


Fig. 8. Emission signals vs. sodium content (in pg) for mixed $NaCl/MgSO_4$ single aerosol particles. Error bars are not shown, but are on the order of $\sim 3\%$ standard error for sodium emission and $\pm 10\%$ for sodium content/particle (as in Figs. 4 and 5).

response, with no apparent salt effects (Fig. 8). Experiments were also carried out with seawater (Fig. 6). Gulf of Mexico seawater (collected in November 1999 on board the R/V Calanus) was filtered through a 0.2 μm filter under vacuum to remove particulates. The filtrate was diluted with MilliQ water to give a set of three solutions with sodium concentrations of 1, 2 and $3 \times 10^{-4}$ M, based on an initial concentration of 10.775 g Na $kg^{-1}$ seawater. The sodium response of the single aerosol seawater particles is also linear, and identical to that from the other sodium salts. Although seawater is a complex mixture of many salts and trace organic and inorganic constituents, the results shown in Fig. 6 indicate that none of these constituents significantly interfere with sodium emission under these conditions.

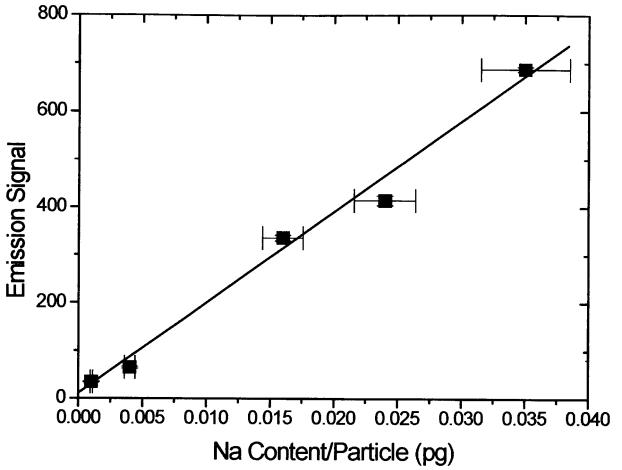


Fig. 9. Emission signal vs. sodium content of a single aerosol particle (in pg) for the high gain PMT. Error bars shown are standard errors for emission signals and $\pm$ 10% for Na mass/particle. The highest and lowest points correspond to NaCl particles of 429 and 300 nm diameter (DMA) respectively (RH $\sim$ 25%).

### 3.3. Low-level detection limits

To determine the low-level detection limit of the ASD, Fig. 9 shows a plot of sodium emission signals as a function of sodium content for sub-micron monodisperse NaCl aerosols generated by the VOAG using a high-gain PMT (Hamamtsu, R3896). NaCl solutions ranged from $1.4 \times 10^{-6}$ to $0.58 \times 10^{-4}$ M NaCl, i.e. a factor of 10–100 times lower sodium concentration than used in the linearity/chemical interference studies. The NaCl aerosol particles produced by the VOAG ranged from 300 to 429 nm in diameter after conditioning in the drying column, as measured by a Differential Mobility Analyzer (TSI 3010; Yeh, 1993). For the most dilute solutions, measured particle sizes were larger than sizes calculated for dry salt particles on the basis of the VOAG size and salt concentration. This difference is attributed to impurities introduced into the salt solutions by glassware and tubing used to deliver solution to the VOAG. The signal : background ratio for the lowest calibration point was $\sim$ 10 : 1 (based on the measured integrated emission signal vs. the average intercept of the sodium calibration curves extrapolated to a sodium concentration of zero). The lowest sodium level measured in this study would correspond to a $\sim$ 100 nm diameter, completely dry, pure NaCl aerosol particle ($1 \times 10^{-3}$ pg Na). This is the detection limit of the ASD in its current configuration.

### 3.4. Ambient aerosols

An ASD was deployed in April 2000 during the SEAS intensive at the University of Hawaii's coastal meteorological research site (Bellows air force base, Hawaii). At this sampling site, winds were consistently out of the East over the ocean at speeds from 6 to 8 m $s^{-1}$ and RH $\sim$ 70–80%, with an off-shore reef break contributing locally to seasalt aerosol production (Tony Clark, University of Hawaii, private communication). An example of typical results from this first field

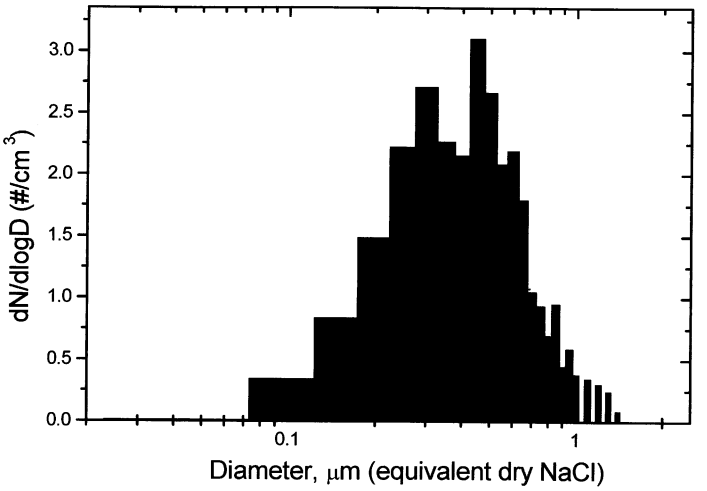


Fig. 10. Sodium-containing particle concentrations vs. diameter as equivalent dry NaCl at 22:03 on April 26 2000 at Bellows Air-Force Base, Oahu, Hawaii. Winds were easterly at $\sim 6$ m s$^{-1}$ and the relative humidity was approximately 75%.

deployment are described below. Ambient aerosols were sampled by the ASD under the same operating conditions used in the previous laboratory tests. Results from an experiment run on April 26, 2000 at 22:03 are shown in Fig. 10. Winds were easterly at 6 m s$^{-1}$, with a relative humidity of approximately 75%. Emission signals were converted to sodium content (in pg) with a four-point NaCl calibration curve. Data are reported as equivalent diameters of dry NaCl aerosol particles.

The maximum in sodium-containing particles is observed between 200 and 800 nm, with a concentration of approximately 1.2 particles cm$^{-3}$ in the entire interval (100 nm–2.0 μm) sensed by the ASD. It should be noted that the particle transmission efficiency through the ASD burner is not included in this estimation, and the actual sodium-containing particle concentration may be higher than given here. The peak maximum in the sodium-containing particles is in contrast to the accumulation mode peak maximum of $\sim$ 100–200 nm measured over the same time period at the same site by the University of Hawaii, with *total* particle concentrations of 100–150 particles cm$^{-3}$ (Tony Clark, private communication). These results suggest that sub-micron seasalt aerosol particles compose just a few percent of the sub-micron aerosol number distribution under the conditions at this site. This is in accord with the low levels of sub-micron sodium-containing particles measured by Hobbs (1971) in the Pacific Ocean off the west coast of the USA at surface wind-speeds of 4 m s$^{-1}$. These field results will be described in detail in a subsequent paper.

## 4. Summary

A single-particle sodium detector (aerosol sodium detector; ASD) has been developed based on thermal sodium emission in hydrogen/air flames. Laboratory experiments with synthetic monodisperse aerosols demonstrate that the ASD has:

- a linear response function over the size range of interest (0.1–2.0 μm diameter);
- precision on the order of $\pm \sim 3\%$ standard error on replicate measurements;
- a quantitative response to the sodium content of a single aerosol particle independent of the chemical composition of the particle, i.e. anions, cations, seawater;
- a lower detection limit of $\sim$100 nm equivalent diameter 100% dry NaCl aerosol.

The ASD can provide *quantitative* near real-time measurements of sodium in single aerosol particles in the sub-micron size range. The ASD will allow us to directly measure the relative importance of seasalt aerosol particles in this size range under a wide range of ambient conditions and to test current models for seasalt aerosol production as a function of wind speed.

## Acknowledgements

The authors gratefully acknowledge funding by the Office of Naval Research (Grant No. N00014-99-1-0031) and thank Cyril McCormick, Warren de Bruyn and Tom Snowden for helpful discussions and generous loan of instrumentation, Rod Zika and the crew of the R/V Calanus for supplying a seawater sample, and Steven Domonkos and Manuel Rodriguez for fine machining of burner components. The authors also thank Tony Clark and Steve Howell at the University of Hawaii for generous assistance with the field experiment during the SEAS intensive in April 2000 in Hawaii.

## References

Alkemade, C. Th. J., & Herrmann, R. (1979a). The flame. In C. Alkemade (ed.) *Fundamentals of analytical flame spectroscopy*. New York: Wiley (Chapter 3).

Alkemade, C. Th. J., & Herrmann, R. (1979b). Pneumatic nebulization, desolvation and voltalization of the analyte. In C. Alkemade (ed.) *Fundamentals of analytical flame spectroscopy*. New York: Wiley (Chapter 4).

Alkemade, C. Th. J., & Herrmann, R. (1979c). Dissociation and ionization of the analyte in the flame. In C. Alkemade (ed.) *Fundamentals of analytical flame spectroscopy*. New York: Wiley (Chapter 5).

Baron, P. A., Mazunder, M., & Cheng, Y. S. (1993). Direct-reading techniques using optical particle detection. In K. Willeke & P. A. Baron (eds.) *Aerosol measurement: Principles, techniques and applications*. New York: Van Nostrand Reinhold (Chapter 17).

Blanchard, D. C. (1983). The production, distribution and bacterial enrichment of the seasalt aerosol. In: P. S. Liss, & W. G. N. Slinn, (Eds.), *Air–sea exchange of gases and particles*. (pp. 407–454). Boston: Reidel.

Blanchard, D. C., & Woodcock, A. H. (1957). Bubble formation and modification in the sea and its meteorological significance. *Tellus*, *9*, 145–158.

Blanchard, D. C., & Woodcock, A. H. (1980). The production, concentration and vertical distribution of the sea-salt aerosol. *Annales of New York Academy Science*, *338*, 330–347.

Chameides, W. L., & Stelson, A. W. (1992). Aqueous-phase chemical processes in deliquescent sea-salt aerosols: A mechanism that couples the atmospheric cycles of S and sea salt. *Journal of Geophysical Research*, *97*(20), 20–565, 580.

Gong, S. L., Barrie, L. A., Blanchet, J.-P., & Spacek, L. (1998). Modeling size-distributed sea salt aerosols in the atmosphere: An application using Canadian climate models. In S.-E. Gryning, & N. Chaumerliac (Eds.), *Air pollution modeling and its applications XII*. New York: Plenum Press.

Hegg, D. A., Hobbs, P. V., Ferek, R. J., & Waggoner, A. P. (1995). Measurements of some aerosol properties relevant to radiative forcing on the East Coast of the United States. *Journal of Applied Meteorology*, *34*, 2306–2315.

Hobbs, P. V. (1971). Simultaneous airborne measurements of cloud condensation nuclei and sodium-containing particles over the ocean. *Quarterly Journal Royal Meteorology Society*, *97*, 263–271.

Hynes, A. J., Steinberg, M., & Schofield, K. (1984). The chemical thermodynamics of sodium species in oxygen-rich flames. *Journal of Chemical Physics*, *80*, 2585–2597.

John, W. (1993). The characteristics of environmental and laboratory-generated aerosols. In K. Willeke, & P. A. Baron (Eds.), *Aerosol measurement: Principles, techniques and applications*. New York: Van Nostrand Reinhold (Chapter 5).

Keene, W. C., Sander, R., Pzenny, A. A. P., Vogt, R., Crutzen, P. J., & Galloway, J. N. (1998). Aerosol pH in the marine boundary layer: A review and model evaluation. *Journal of Aerosol Science*, *29*, 339–356.

Livingston, F. E., & Finlayson-Pitts, B. J. (1991). The reaction of gaseous $N_2O_5$ with solid NaCl at 298 K: Estimated lower limit to the reaction probability and its potential role in tropospheric and stratospheric chemistry. *Geophysical Research Letters*, *18*, 17–20.

Monahan, E. C., Spiel, D. E., & Davidson, K. L. (1986). Model of marine aerosol generation via whitecaps and wave disruption in oceanic whitecaps. In: E. C. Monahan, & G. M. Niocaill, (Eds.), *Oceanic whitecaps and their role in air–sea exchange processes* (pp. 167–174). Dordrecht Holland: Reidel.

Murphy, D. M., Anderson, J. R., Quinn, P. K., McInnes, L. M., Brechtel, F. J., Kreidenweis, S. M., Middlebrook, A. M., Posfai, M., Thomson, D. S., & Bruseck, P. R. (1998a). Influence of sea-salt on aerosol radiative properties in the Southern Ocean marine boundary layer. *Nature*, *392*, 62–65.

Murphy, D. M., Thomson, D. S., Middlebrook, A. M., & Schein, M. E. (1998b). In situ single-particle characterization at Cape Grim. *Journal of Geophysical Research*, *103*(16), 16–485, 491.

O'Dowd, C. D., & Smith, M. H. (1993). Physicochemical properties of aerosols over the Northeast Atlantic: Evidence for wind-speed related sub-micron sea-salt aerosol production. *Journal of Geophysical Research*, *98*, 1137–1149.

O'Dowd, C. D., Smith, M. H., Consterdine, I. E., & Lowe, J. A. (1997). Marine aerosol, sea-salt, and the marine sulphur cycle: A short review. *Atmospheric Environment*, *31*, 73–80.

Radke, L. F., & Hobbs, P. V. (1969). Measurement of cloud condensation nuclei, light scattering coefficient, sodium-containing particles, and aitken nuclei in the Olympic Mountains of Washington. *Journal of Atmospheric Science*, *26*, 281–288.

Sievering, H., Boatman, J., Gorman, E., Kim, Y., Anderson, L., Ennis, G., Luria, M., & Pandis, S. (1992). Removal of sulfur from the marine boundary layer by ozone oxidation in sea-salt aerosols. *Nature*, *360*, 571–573.

Soudain, G. (1951). Realisation d'un compteur automatique de noyaiux de chlorure de sodium. *Journal of Science and Meteorology*, *3*, 137–142.

Vonnegut, B., & Neubauer, R. L. (1953). Counting sodium-containing particles in the atmosphere by their spectral emission in a hydrogen flame. *Bulletin of American Meteorology Society*, *34*, 163–169.

Woodcock, A. H. (1953). Salt nuclei in marine air as a function of altitude and wind force. *Journal of Meteorology*, *10*, 362–371.

Yeh, H.-C. (1993). Electrical Techniques. In K. Willeke & P. A. Baron (eds.) *Aerosol measurement: Principles, techniques and applications*. New York: Van Nostrand Reinhold (Chapter 18).

Zeegers, P. J. T., Smith, R., & Winefordner, J. D. (1968). Shapes of analytical curves in flame spectrometry. *Annales of Chemistry*, *40*, 26A–47A.